



4-Iodophenylboronic Acid Stabilized Gold Cluster as a New Fluorescent Chemosensor for Saccharides Based on Excimer Emission Quenching

Jaydev Thakarda¹ · Pranav Dave¹ · Sagar Bhowmik¹ · Jasmin Kubavat¹ · Prasenjit Maity¹ 

Received: 16 October 2020 / Accepted: 28 December 2020 / Published online: 8 January 2021

© The Author(s), under exclusive licence to Springer Science+Business Media, LLC part of Springer Nature 2021

Abstract

4-iodophenylboronic acid (IPBA) ligated luminescent gold cluster was synthesized by mixing an aqueous solution of IBPA and polyvinylpyrrolidone stabilized gold cluster (Au:PVP) in water at room temperature through chemisorption of iodine on gold nano surface. Transmission Electron microscopy (TEM) and matrix assisted laser desorption ionization (MALDI) analysis revealed that the size of these Au-clusters (1.4 ± 0.2 nm) remain unchanged without any noticeable aggregation during synthesis. Owing to the formation of excimer between aryl moieties grafted over Au surface, the cluster exhibit strong emission peak at 335 nm. This luminescent gold cluster is used for sensing different saccharides in water at physiological pH through quenching of excimer emission peak. This strong excimer emission is significantly quenched in presence of saccharides through interaction with boronic acid moieties. The selectivity for different saccharides follows the order: fructose > galactose > maltose > glucose ~ ribose > sorbitol with high affinity for fructose ($K_{SV} = 1.54 \times 10^4 \text{ M}^{-1}$) with Limit of Detection (LOD) of 100 μM .

Keywords 4-Iodophenylboronic acid · Gold cluster · Excimer · Chemosensor · Saccharides

Introduction

The development of new fluorescent chemosensor is of paramount interest in analytical chemistry from both its fundamental mechanistic viewpoint and possibility of its real-world application. Selective detection and quantification of saccharide molecules has wide applicability due to their innumerable biological role as nature's conveyors of energy for cell survival [1]. The composition of several packaged food products includes specific saccharide molecules and hence monitoring food quality also demands easy to use saccharide sensors [2]. Continuous monitoring of blood sugar level is very important for diabetic patients and thus further signifies its necessity [3]. The different strategies validated for saccharide sensing includes enzyme-based method [4], electrochemical technique

[5], optical rotation [6], near infrared spectroscopy [7], colorimetric detection [8] and luminescence-based detection [9]. Every technique has its own merits and demerits in terms of sample processing, time of analysis, cost and accuracy. Enzyme-based method is more commonly used in pathological laboratories for blood and urine glucose measurement purposes due to its accuracy and reliability, however it should be noted that this technique is comparatively costly, not feasible for onsite testing and inconvenient for continuous glucose monitoring purposes. Fluorescence based method for saccharide sensing is gaining popularity because of its many advantages including fast response, ultra-low detection limit, relatively cheap, onsite testing feasibility and ease of continuous monitoring [9]. Aryl boronic acids are preferred choices as fluorescent chemosensor for detection of saccharides due to ease of chemical adduct formation between boronic acid and cis-diol moiety of saccharides [9–15]. The initial pioneering works of Czarnik [14] and Shinaki [15] has popularised the applications of aryl boronic acid derivatives as fluorescent chemosensors for several vicinal diols including saccharides as these compounds bind with boronic acids through reversible ester formation. In last four decades several aryl boronic acid derivatives containing benzene, naphthalene,

✉ Jasmin Kubavat
kubavatjasmin@gfsu.edu.in

✉ Prasenjit Maity
pmaity@gfsu.edu.in

¹ School of Engineering and Technology, National Forensic Sciences University, Sect or-09, Gandhinagar 382007, India

phenanthrene, anthracene, pyrene, fluorene, porphyrin, as well as various heterocyclic aromatic groups have been used [9–15]. Tedious synthetic procedure, use of mixed solvent due to lack of water solubility and selectivity are some of the drawbacks which needs attention in this field. The application of carbon dot [16], semiconductor quantum dot [17] and protein stabilized gold nanoclusters [18] based fluorescent sensors has also been recently reported for sensing saccharides.

Luminescent gold clusters are an important class of “*functional nanomaterials*” due to their many potential applications including detection of trace level analytes and in the emerging areas of bio-imaging [19–21]. The synthetic simplicity, air stability and more importantly their biocompatibility (nontoxic nature) makes them so promising for both in vivo and in vitro imaging and sensing applications. Luminescent gold clusters with thiol [22, 23], alkyne [24, 25], carbene, [26] protein [18, 27] and dendrimer [28] based ligands have been reported with very distinct origin of fluorescence for each category. Detection of heavy metals [20], explosives [29], bio-molecules [30], drugs and psychotropic substances [31], pesticides [32] and food pathogens [33] have been demonstrated by using various fluorescent gold clusters and nanoparticles. Although some advances have been made, but luminescent gold clusters with tuneable emission wavelength, large scale synthesis possibility, easy surface modification for desired solubility and selective analyte binding specificity are still lacking in this field. Recently aryl iodide ligated mixed ligand stabilized gold cluster was reported by few of us, where strong excimer-based fluorescence was observed [34]. These clusters are fundamentally very interesting because poorly fluorescent aryl iodides with strong heavy atom effect becomes highly emissive through excimer formation when grafted over gold nano surface. We believe that in real application front these clusters will be superior as compared to other ligand protected gold clusters due to following specialities of this cluster: (i) tuneable emission wavelength based on aryl iodide ancillary ligands, (ii) feasibility of large scale synthesis by simple mixing strategy under ambient conditions, (iii) ease of tuning surface functional groups for selective sensing of a particular analyte. Combining the well-known binding interaction between boronic acid moiety and saccharides and our newly explored synthesis of aryl iodide stabilized luminescent gold cluster we thought to develop a chemosensor in the form of 4-iodophenylboronic acid stabilized gold cluster for saccharide sensing (Scheme 1).

Thus, in the present work, we report synthesis of 4-iodophenylboronic acid and polyvinylpyrrolidone mixed ligand stabilized fluorescent gold cluster and its application for sensing of saccharides in water at neutral pH conditions. The cluster showed strong fluorescence property due to excimer emission of aryl groups grafted on gold and upon addition of saccharide a chemical interaction with boronic acid causes extensive quenching of this

excimer emission. The cluster showed linear response to a range of monosaccharides in the concentration range of 4–12 mM with very low detection limit up to 100 μ M.

Experimental

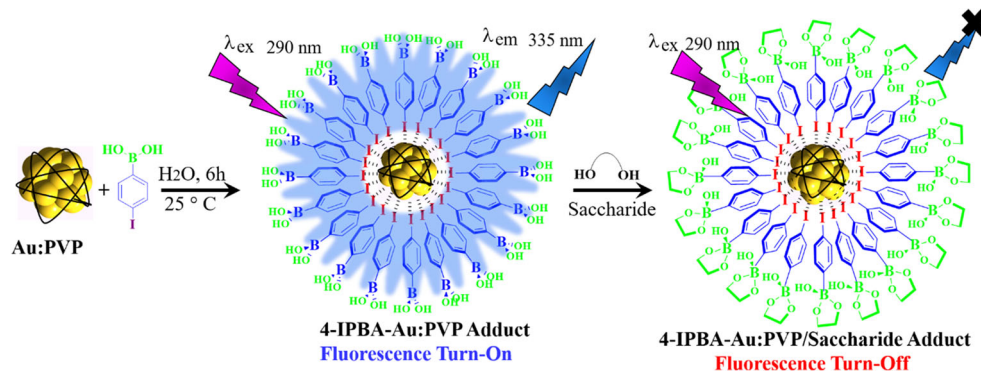
Materials and Instruments

All the reagents and solvents were procured from commercial sources and used without further purification unless otherwise mentioned (Sigma-Aldrich Chemical Co. and S D Fine Chemicals). Optical (UV–Vis) spectra were recorded in a JASCO V-670 spectrophotometer at 298 K. Solution phase fluorescence spectra were obtained by using a JASCO FP-6500 spectrophotometer at 298 K. Transmission electron microscopic (TEM) images were recorded by using a Philips JEM 2000FX electron microscope operated at 200 kV. An aqueous dispersion of Au-cluster was drop-casted onto hydrophilic carbon-coated copper grids followed by drying at ambient conditions before their loading in electron microscope. Dynamic light scattering (DLS) experiments for measuring hydrodynamic diameter of Au-clusters were performed by using a Malvern DLS instrument (Zetasizer Nano ZSP model). MALDI mass spectra of gold clusters were recorded by using a time-of-flight (TOF) mass spectrometer (Bruker, Autoflex Speed) operated with a solidstate laser (355 nm, 3 Hz, <100 mJ). Au:PVP or IPBA-Au:PVP samples (1 mg) were dispersed in water (50 μ L) in a glass vial and *trans*-2-[3-(4-*tert*-Butylphenyl)-2-methyl-2-propenyldene]malononitrile (DCTB, 1 mg) was dissolved in 50 μ L methanol in another vial. Then these two solutions were mixed and drop casted on a stainless steel MALDI plate followed by their drying under open air. Then the MALDI plate was inserted inside mass spectrometer for measurement. Time resolved fluorescence lifetime measurements of the gold clusters with and without addition of saccharide were performed by using a picosecond time-correlated single photon counting (TCSPC) instrument (Edinburgh Instruments Ltd., Lifespec II model), where a 300 nm excitation source was used and data collected at 335 nm emission wavelength. The IBH DAS 6.0 software was used to analyze the lifetime decays by the iterative reconvolution method.

Synthesis of au:PVP Cluster

An aqueous solution of HAuCl₄ (1 mM, 30 mL) was mixed with PVP (K30, 0.6 mmol in monomer unit) and the mixture was stirred for 15 min at 273 K. Then Au:PVP (1.4 nm) nanoparticle was obtained by mixing the fresh aqueous solutions of HAuCl₄/PVP with NaBH₄ (0.1 M, 3 mL) at 273 K under vigorous stirring for 30 min. Then this dispersed aqueous Au:PVP nanoparticle was purified by ultrafiltration with membrane filter (10 kDa Mol. Wt. cut of limit) for a prolonged

Scheme 1 Synthetic route of 4-iodophenylboronic acid ligated Au-nanocluster (IPBA-Au:PVP) and schematic representation of sensing mechanism involves in supramolecular adduct with saccharides



time at 280 K. Finally, the analytically pure powdered Au:PVP (1.4 nm) nanoparticle was obtained by lyophilizing the deionized dispersion of as-synthesized Au:PVP nanoparticle obtained through ultrafiltration using a fridge dryer [35].

Synthesis of IPBA-au:PVP Cluster

The 4-iodophenylboronic acid (IPBA) attached Au:PVP nanocluster (IPBA-Au:PVP) was synthesized by simply mixing IPBA ligand and Au:PVP cluster in water at 298 K for 6 h (Scheme 1). In brief, first a 10 mL stock solution of IPBA (1 mM in Methanol) and a 10 mL stock solution of Au:PVP cluster (1 mM in water) cluster were prepared. Then 1 mL of IPBA stock solution and 0.5 mL of Au:PVP stock solution was mixed in a vial and additional 9 mL water was added under stirring at 298 K for 6 h to get the final IPBA-Au:PVP cluster. The solution was also lyophilized in a fridge dryer to get it in fine powders form which could be preserved for use in future. The duplicate solutions with identical concentrations of only IPBA and only Au:PVP were also prepared for comparison of their spectral profiles.

Saccharide Sensing by Fluorescence Titration

To evaluate the sensing performance of IPBA-Au:PVP nanocluster, fluorescence titration experiments were performed against a series of saccharides (fructose, ribose, glucose, galactose, sorbitol and maltose) in water at neutral pH (7.5) at 298 K. All the emission spectroscopic measurements were performed by using excitation wavelength (λ_{ex}) of 290 nm and the corresponding emission wavelength at 335 nm was monitored. For each measurement, 2 mL aqueous solution of as prepared IPBA-Au:PVP cluster was taken in cuvette and titrated against incremental addition of aqueous saccharide solution (20 μL each time from a concentrated stock solution with concentration of 100 mM). The pH of measured solutions was monitored by using a digital pH meter (Metrohm model no. 780). The variation of emission profile of aqueous IPBA-Au:PVP cluster with varying pH values

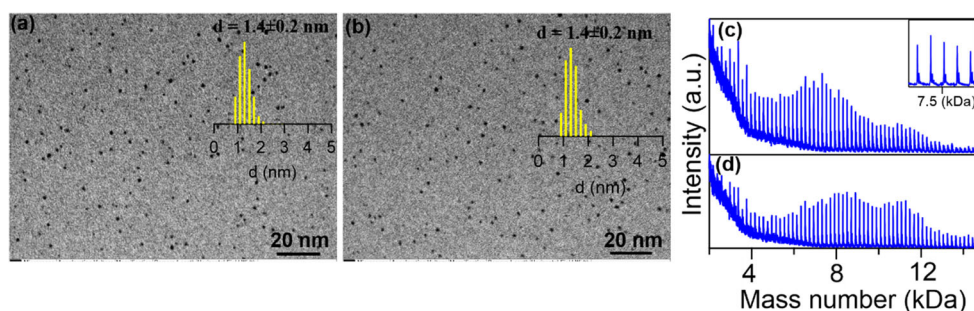
were measured in the range of 2–12 by adjusting pH with HCl or NaOH additions.

Results and Discussion

Synthesis and Characterization of Fluorescent au Cluster

The fluorescent gold nanocluster (IPBA-Au:PVP) under present study was prepared via a straight forward synthetic method as reported by few of us by mechanical mixing of 4-iodophenylboronic acid ancillary ligand with Au:PVP nanocluster in water, incubated for 6 h at 298 K (Scheme 1)[34]. Initially we have carried out transmission electron microscope (TEM) and MALDI mass analysis of both precursor Au:PVP cluster and IPBA-Au:PVP cluster as shown in Fig. 1. The particle size distribution of precursor Au:PVP cluster and IPBA-Au:PVP nanocluster is very identical as both show 1.4 ± 0.2 nm size in their respective TEM image analysis (Fig. 1a,b). Mass spectrometric analysis of gold clusters gives more accurate measurement by giving number of gold atoms in the clusters [36]. We measured the mass spectral profiles of both gold clusters by using DCTB as matrix in a MALDI TOF setup (Fig. 1c,d). The highest intensity peak at 8 kDa in Au:PVP cluster suggest ~ 40 gold atom based cluster ($\sim \text{Au}_{40}$) is the major constituent in it. However, the mass spectra of IPBA-Au:PVP showed two maxima points at 8 and 11 kDa values, which implies along with $\sim \text{Au}_{40}$ cluster, $\sim \text{Au}_{55}$ cluster is also present in it. The result indicates little increase of gold cluster size during its solution phase synthesis although it is difficult to notice through TEM measurement. The average hydrodynamic diameter (D_h) for both Au:PVP and IPBA-Au:PVP clusters dispersed in water were also measured by dynamic light scattering (DLS) technique to get an idea about their solution phase behaviour and stabilities. We observed that their hydrodynamic diameter is also very identical (~ 11 nm) indicating well dispersed individual Au-clusters in water (Fig. 2a,b). To gain more insight into the long term solution (aqueous) phase stability and aggregation

Fig. 1 TEM images with particle size histograms (a and b) and MALDI mass spectra (c and d) of Au:PVP precursor cluster and IPBA-Au:PVP cluster respectively. The inset in (c) shows that each individual peak in the mass spectra corresponds to a particular gold cluster with a single gold atomic mass (197 Da) difference between two peaks



behaviour of IPBA-Au:PVP cluster, a time dependent size (hydrodynamic diameter, D_h) measurement was performed up to 48 h. The result revealed identical particle size distribution during the said period indicating stability of IPBA-Au:PVP in aqueous phase for long term. (Figure S1).

Photophysical Properties of IPBA-au:PVP Nanocluster

The solution phase optical (UV-Vis) and fluorescence spectral profiles of IPBA, Au:PVP and IPBA-Au:PVP clusters were recorded in water at 298 K (Fig. 3a,b). The Au:PVP cluster exhibits a characteristics exponential absorption profile in the UV region ($400 \rightarrow 200$ nm) which is originated from $5d \rightarrow 6sp$ electronic transition [37]. However, the pristine IPBA ligand show a characteristic absorption peak at 240 nm and in IPBA ligated Au:PVP cluster the absorption peak is slightly enhanced indicating adsorption of the ligand on gold surface through some electronic interaction. The emission spectra of IPBA shows only a weak peak at 307 nm due to the presence of heavy atom (iodine) and as we have reported previously, Au:PVP cluster have no detectable fluorescence [34]. However, the synthesized IPBA-Au:PVP cluster showed a strong emission peak centred at 335 nm ($\lambda_{max} = 290$ nm)

was observed (Fig. 3b). 3d emission profile of the cluster (Fig. S2) was also recorded to confirm the exact excitation and emission wavelengths. This highly enhanced emission peak at 335 nm is originated due excimer formation of aryl groups grafted on gold surface. Here the rate of excimer formation is much faster as compared to intersystem crossing process of aryl iodide ligand although a heavy atom (Iodine) is present in it [34].

Fluorescence Sensing of Saccharides

To find the efficacy of IPBA-Au:PVP cluster for saccharide sensing, steady-state fluorescence titrations were conducted against a range of saccharide molecules (fructose, ribose, glucose, galactose, sorbitol and maltose) with IPBA-Au:PVP nanocluster in water at physiological pH (7.5) at 298 K. We could anticipate that saccharide molecules will interact with boronic acid group and a fluorescence response will be observed (Scheme 1). Initially we conducted the fluorescence titration of glucose with the gold cluster by gradual addition of increasing amount of glucose (typically, 20 μ L of 100 mM solution in water at a time) to the gold nanocluster solution (2 mL of 100 μ M in water) in a cuvette. The fluorescence peak

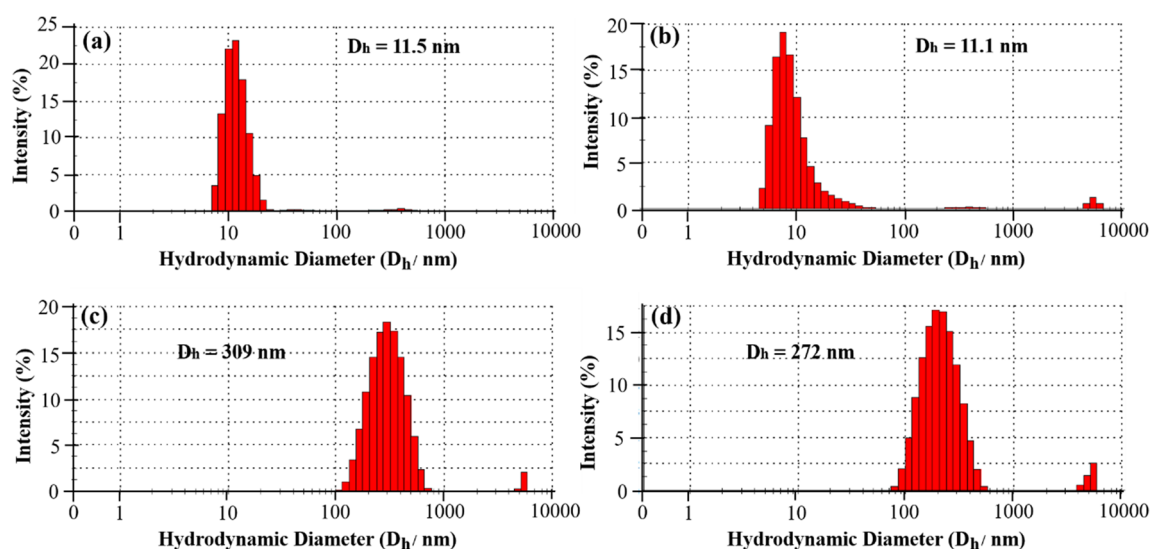
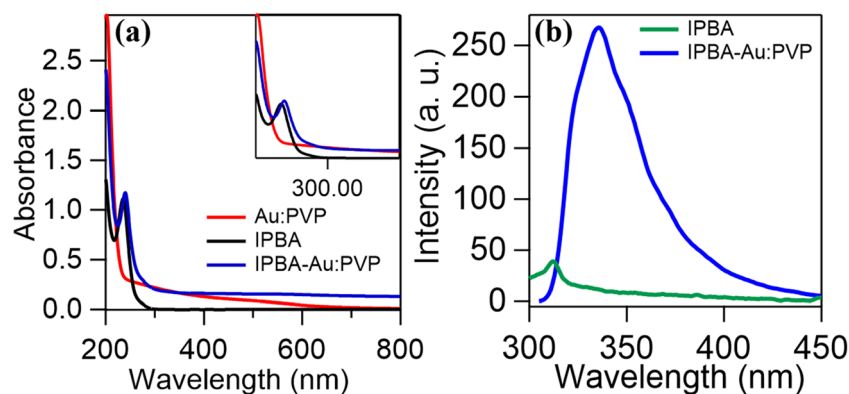


Fig. 2 Hydrodynamic diameter (D_h) of Au:PVP cluster (a); IPBA-Au:PVP nanocluster (b); IPBA-Au:PVP nanocluster after titration with fructose (c) and IPBA-Au:PVP nanocluster after titration with galactose respectively, in water at 298 K at neutral pH

Fig. 3 Comparative UV–Vis spectra (a) and fluorescence spectra (b) of IPBA ligand, Au:PVP nanocluster and IPBA–Au:PVP nanocluster, respectively, in water at 298 K



at 335 nm gradually decreases with sequential addition glucose (Fig. 4b) and the result clearly demonstrate the sensing ability of our gold cluster for saccharides. Interestingly, we could also observe that the intensity of 240 nm peak in the UV-Vis absorption profile of IPBA–Au:PVP cluster increases along with the enhancement of an absorption band at 300 nm (Fig. 4a). This observation probably arises due to electronic exchange between iodophenylboronic acid and glucose through formation of boronic ester. Next, we have studied the fluorescence titration with another five saccharide molecules (fructose, ribose, galactose, sorbitol and maltose) under identical experimental conditions to find out the comparative sensing performance of the gold cluster. As can be seen (Fig. 5a–e) the excimer-based emission of IPBA–Au:PVP nanocluster significantly quenched upon addition of all these different saccharide molecules. To evaluate the sensing efficiency, we plotted normalized emission intensity (I_0/I) against concentrations of added saccharide molecules by following the Stern-Volmer equation (Fig. 5f) [38].

$$I_0/I = K_{SV}[A] + 1 \quad (1)$$

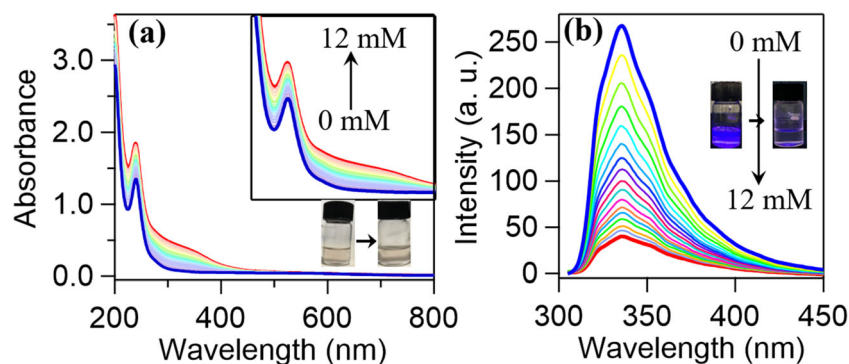
where, I_0 and I are the fluorescence intensities in the absence and presence of saccharide, $[A]$ is the molar concentration of the saccharide, and K_{SV} is the quenching constant (in M^{-1}). The detection limit for all the tested analytes were also calculated by considering 3 times of signal to noise ratio during their respective titrations. Although very low concentrations of saccharides could be detected, but the (I_0/I) against concentrations does fit linearly throughout the whole concentrations range tested by us (0–12 mM), possibly due to complex interaction pattern of boronic acid functionalized gold cluster and saccharides (Fig. 5f). Hence we further plotted the relative emission intensity (I_0/I) against concentration of saccharides in the upper concentration range of 4–12 mM, (Fig. S8) with good linear correlation and the corresponding Stern-Volmer Constant (K_{SV}) and R^2 values are summarized in Table 1. As we could find the K_{SV} values follows the order: fructose > galactose > maltose > glucose ~ ribose > sorbitol with highest K_{SV} obtained for fructose ($1.5 \times 10^4 M^{-1}$) along with very low detection limit of 100 μM . The extent of fluorescence

quenching of the IPBA–Au:PVP cluster caused by adding 12 mM of different saccharides (I_0/I) are also calculated and shown in Fig. 6. The difference of quenching efficiencies of these saccharides may originate due to differences in their binding strengths with the boronic acid moiety due to different dihedral angles of diols of these sugars. We have also performed fluorescence quenching efficiencies (I_0/I) caused by common inorganic salts, e.g., NaCl, KBr, $Fe(NO_3)_3$, NH_4Cl and Na_2SO_4 , as some of these are present in blood and urine (Fig. 6 and Fig. S3). All these salts have very minimal effect on fluorescence quenching with (I_0/I) value within the limit of 1.2 only whereas for the six saccharide molecules these values are much higher: fructose (19.5), galactose (16.5), maltose (9.8), glucose (7), ribose (6.99), sorbitol (4). With these findings we could propose that our synthesized gold cluster could be used as fluorescent chemosensor for detection and quantification of saccharides from different aqueous media provided it does not contain any fluorescent contaminant with similar emission characteristics. Fluorescence lifetime decay studies of IPBA–Au:PVP nanocluster with and without fructose (5 mM) addition were carried out to further understand the sensing mechanism (Fig. S4 and Table S1). A 300 nm excitation wavelength was used and emission decay profile at 335 nm was monitored. The lifetime decay curve of IPBA–Au:PVP cluster was resolved through bi-exponential fitting with average lifetime value of 7.66 ns. Upon addition of

Table 1 Stern-Volmer constants, limit of detection and correlation coefficient of different saccharides obtained from their fluorescence titration with gold cluster in the concentration range of 4–12 mM of saccharides

| Saccharide | K_{SV} | R^2 | LOD | Linear Range |
|------------|---------------------------|--------|-------------|--------------|
| Fructose | $1.50 \times 10^4 M^{-1}$ | 0.99 | 100 μM | 4–12 mM |
| Galactose | $4.2 \times 10^3 M^{-1}$ | 0.9632 | 180 μM | 4–12 mM |
| Maltose | $3.7 \times 10^3 M^{-1}$ | 0.9809 | 200 μM | 4–12 mM |
| Glucose | $2.6 \times 10^3 M^{-1}$ | 0.9798 | 350 μM | 4–12 mM |
| Ribose | $1.5 \times 10^3 M^{-1}$ | 0.9787 | 300 μM | 4–12 mM |
| Sorbitol | $8.1 \times 10^2 M^{-1}$ | 0.9678 | 600 μM | 4–12 mM |

Fig. 4 Titration of IPBA-Au:PVP nanocluster with incremental addition of glucose (0.9 mM to 12 mM) in water at pH 7.5 at 298 K and the corresponding change in UV-Vis spectra (a) and fluorescence spectra (b); inset pictures show visual change of the aqueous gold cluster solution before and after addition of 12 mM glucose under normal day light (a) and under 254 nm UV light (b)



fructose (5 mM) the steady state fluorescence spectra although showed almost 80% quenching (Fig. 5b), but we find no appreciable change in its fluorescence lifetime values ($\tau=7.55$ ns). Thus, we hypothesized that the quenching process is definitely a static quenching process through the formation of stable non-fluorescent ground state adduct of saccharide and IPBA-Au:PVP clusters as shown in scheme 1.

pH Effect and Dynamic Light Scattering (DLS) Experiments

The effect of pH on emission behaviour and saccharide sensing performance were also evaluated by doing the measurements in the pH range of 2–12 in water at 298 K. In the acidic medium the emission wavelength (335 nm) of IPBA-Au:PVP does not shift but its intensity decreases slightly (4%) on

decreasing the pH from 7.5 to 2 (Fig. S5). However, under basic medium the emission peak is broadened and redshifted gradually from 335 nm to 370 nm as well as its intensity also decreases substantially (65%) on increasing the pH from 7.5 to 12 (Fig. S5). Hydrodynamic diameters (D_h) of IPBA-Au:PVP cluster were measured before and after addition of different saccharides (12 mM) after completion of the fluorescence titration and those are shown in Fig. 2 and in Fig. S6. As can be seen the D_h value of the IPBA-Au:PVP nanocluster substantially increases from 11 nm to more than 250 nm after forming adduct with different saccharide molecules. The TEM image analysis of IPBA-Au:PVP gold cluster (Fig. S7) after titration with glucose (12 mM) showed mean size of 1.4 nm, which is very identical with its size distribution before the fluorescence titration (Fig. 1b). Hence, we propose that the increase of hydrodynamic diameter (D_h) of the gold cluster

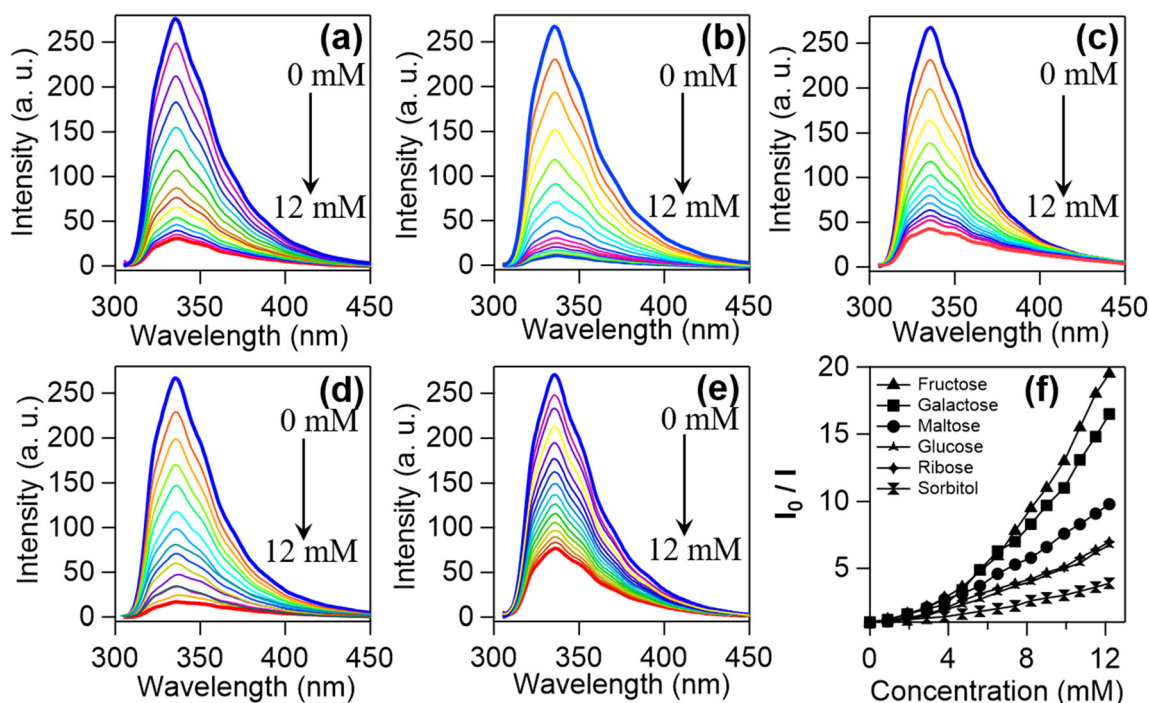


Fig. 5 Fluorescence spectroscopic titration of IPBA-Au:PVP nanocluster with incremental addition (0.9 mM to 12 mM) of a maltose, b fructose, c ribose, d galactose and e sorbitol, respectively, in water at 298 K under

neutral pH of 7.5. f Stern-Volmer plots obtained from each individual fluorescence spectroscopic titration experiments

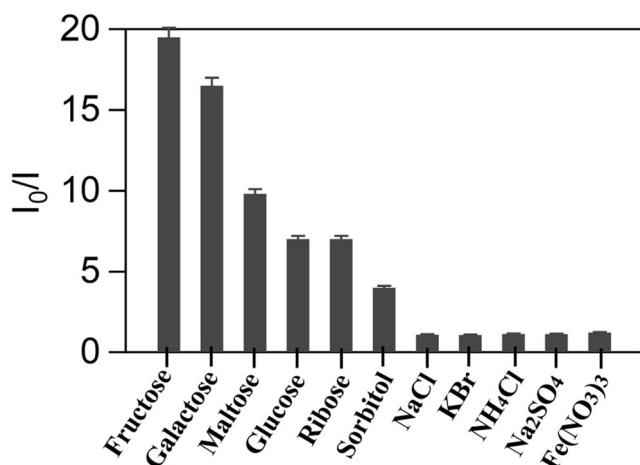


Fig. 6 The representative ‘bar diagram’ showing the fluorescence quenching efficiency (I_0/I) of different saccharides and inorganic salts obtained from fluorescence titration with IPBA-Au:PVP nanocluster in water at 298 K after addition of 12 mM of each analytes. The error bars are within 3% limit

after its derivatization with saccharide is due to lose aggregate formation between individual gold clusters through hydrogen bond formation between outer saccharide molecules (Scheme S1).

Conclusions

In summary, we have synthesized a new luminescent Au-nanocluster (viz. IPBA-Au:PVP) through grafting 4-iodophenylboronic acid on the surface of preformed gold cluster by a simple solution phase incubation strategy with high efficiency as compared to common organic chemosensors (Table S2). This IPBA-Au:PVP cluster exhibits strong fluorescence property originated from excimer emission, although the corresponding free ligand (IPBA) is non luminescent due to the presence of iodine (heavy atom effect). Aqueous phase detection of various saccharide molecules was performed at neutral pH (7.5) with micromolar detection limit through quenching of excimer emission of this Au-nanocluster. The selectivity for different saccharides follows the order fructose > galactose > maltose > glucose ~ ribose > sorbitol with high affinity for fructose ($K_{SV} = 1.54 \times 10^3 \text{ M}^{-1}$) with Limit of Detection (LOD) of 100 μM . The work presents first state of the art demonstration of a luminescent ultrasmall gold cluster as fluorescent chemosensor for different saccharides in water.

Supplementary Information The online version contains supplementary material available at <https://doi.org/10.1007/s10895-020-02672-2>.

Author Contributions JT, PD, SB synthesized and characterized the nanocomposite and did all the sensing studies using spectrofluometry, SB performed MALDI mass measurements, JK and PM conceptualized the work and wrote the paper.

Funding This work was supported by Council of Scientific & Industrial Research (CSIR, New Delhi) (Project no. 01(2873)/17/EMR-II).

Data Availability The authors declare that the data supporting the findings of this study are available in the article and in the supplementary materials.

Compliance with Ethical Standards

Conflict of Interest The authors declare no conflict of interest.

References

- Patel V (2019) Molecular nutrition: Carbohydrates. Academic Press, Cambridge
- Popkin BM, Hawkes C (2016) Sweetening of the global diet, particularly beverages: patterns, trends, and policy responses. *Lancet Diabetes Endocrinol* 4:174–186. [https://doi.org/10.1016/S2213-8587\(15\)00419-2](https://doi.org/10.1016/S2213-8587(15)00419-2)
- Vashist SK (2012) Non-invasive glucose monitoring technology in diabetes management: a review. *Anal Chim Acta* 750:16–27. <https://doi.org/10.1016/j.aca.2012.03.043>
- D’Auria S, Dicesare SN, Gryczynski Z, Gryczynski I, Rossi M, Lakowicz JR (2000) A thermophilic apoglucose dehydrogenase as nonconsuming glucose Sensor. *Biochem Bioph Res Co* 274: 727–731. <https://doi.org/10.1006/bbrc.2000.3172>
- Noiphung J, Songjaroen T, Dungchai W, Henry CS, Chailapakul O, Laiwattanapaisal W (2013) Electrochemical detection of glucose from whole blood using paper-based microfluidic devices. *Anal Chim Acta* 788:39–45. <https://doi.org/10.1016/j.aca.2013.06.021>
- Rabinovitch B, March WF, Adams RL (1982) Noninvasive glucose monitoring of the aqueous humor of the eye: Part I. Measurement of very small optical rotations. *Diabetes Care* 5:254–258. <https://doi.org/10.2337/diacare.5.3.254>
- Robinson MR, Eaton RP, Haaland DM, Koeppe GW, Thomas EV, Stallard BR, Robinson PL (1992) Noninvasive glucose monitoring in diabetic patients: a preliminary evaluation. *Clin Chem* 38:1618–1622
- Palazzo G, Facchini L, Mallardi A (2012) Colorimetric detection of sugars based on gold nanoparticle formation. *Sensor Actuat B-Chem* 161:366–371. <https://doi.org/10.1016/j.snb.2011.10.046>
- Caol H, Heagy MD (2004) Fluorescent chemosensors for carbohydrates: a decade’s worth of bright spies for saccharides in review. *J Fluoresc* 14:569–584. <https://doi.org/10.1023/B:JOFL.0000039344.34642.4c>
- Zhang Y, He Z, Li G (2010) A novel fluorescent vesicular sensor for saccharides based on boronic acid–diol interaction. *Talanta* 81: 591–596. <https://doi.org/10.1016/j.talanta.2009.12.041>
- Hosseinzadeh R, Mohadjerani M, Pooryousef M, Eslami A, Emami S (2015) A new boronic acid fluorescent sensor based on fluorene for monosaccharides at physiological pH. *Spectrochim Acta A* 144: 53–60. <https://doi.org/10.1016/j.saa.2015.02.066>
- Ni N, Laughlin S, Wang Y, Feng Y, Zheng Y, Wang B (2012) Probing the general time scale question of boronic acid binding with sugars in aqueous solution at physiological pH. *Bioorg Med Chem* 20:2957–2961. <https://doi.org/10.1016/j.bmc.2012.03.014>
- Jin S, Zhu C, Li M, Wang B (2009) Identification of the first fluorescent α -amidoboronic acids that change fluorescent properties upon sugar binding. *Bioorg Med Chem Lett* 19:1596–1599. <https://doi.org/10.1016/j.bmcl.2009.02.011>
- Yoon J, Czarnik AW (1992) Fluorescent chemosensors of carbohydrates. A means of chemically communicating the binding of

- polyols in water based on chelation-enhanced quenching. *J Am Chem Soc* 114:5874–5875. <https://doi.org/10.1021/ja00040a067>
15. Sandanayake KRAS, Shinkai S (1994) Novel molecular sensors for saccharides based on the interaction of boronic acid and amines: saccharide sensing in neutral water. *J Chem Soc Chem Commun*: 1083–1084. <https://doi.org/10.1039/C39940001083>
 16. Shehab M, Ebrahim S, Soliman M Graphene quantum dots prepared from glucose as optical sensor for glucose. *J Lumin* 184: 110–116. <https://doi.org/10.1016/j.jlumin.2016.12.006>
 17. Wu W, Zhou T, Berliner A, Banerjee P, Zhou S (2010) Glucose-mediated assembly of phenylboronic acid modified CdTe/ZnTe/ZnS quantum dots for intracellular glucose probing. *Angew Chem Int Ed* 49:6554–6558. <https://doi.org/10.1002/anie.201001508>
 18. Feng D-Q, Chen M, Liu G, Zhu W, Sun W, Zhu R, Wang W (2015) A novel resonance light scattering sensing for glucose based on the conversion of gold nanoclusters into gold nanoparticles. *Sensor Actuat B-Chem* 219:133–138. <https://doi.org/10.1016/j.snb.2015.05.019>
 19. Cui M, Zhao Y, Song Q (2014) Synthesis, optical properties and applications of ultra-small luminescent gold nanoclusters. *Trends Anal Chem* 57:73–82. <https://doi.org/10.1016/j.trac.2014.02.005>
 20. Chansuvarn W, Tuntulani T, Imyim A (2015) Colorimetric detection of mercury (II) based on gold nanoparticles, fluorescent gold nanoclusters and other gold-based nanomaterials. *Trends Anal Chem* 65:83–96. <https://doi.org/10.1021/ac1021503>
 21. Huang Y, Fuksman L, Zhang J (2018) Luminescence mechanisms of ultrasmall gold nanoparticles. *Dalton Trans* 47:6267–6273. <https://doi.org/10.1039/C8DT00420J>
 22. Yu Y, Luo Z, Chevrier DM, Leong DT, Zhang P, Jiang D, Xie J (2014) Identification of a highly luminescent Au₂₂(SG)₁₈ nanocluster. *J Am Chem Soc* 136:1246–1249. <https://doi.org/10.1021/ja411643u>
 23. Pyo K, Thanthirige VD, Yoon SK, Ramakrishna G, Lee D (2016) Enhanced luminescence of Au₂₂(SG)₁₈ nanoclusters via rational surface engineering. *Nanoscale* 8:20008–20016. <https://doi.org/10.1039/C6NR07660B>
 24. Maity P, Takano S, Yamazoe S, Wakabayashi T, Tsukuda T (2013) Binding motif of terminal alkynes on gold clusters. *J Am Chem Soc* 135:9450–9457. <https://doi.org/10.1021/ja401798z>
 25. Ito S, Takano S, Tsukuda T (2019) Alkynyl-protected Au₂₂(C≡CR)₁₈ clusters featuring new interfacial motifs and R-dependent photoluminescence. *J Phys Chem Lett* 10:6892–6896. <https://doi.org/10.1021/acs.jpcclett.9b02920>
 26. Narouz MR, Takano S, Lummis PA, Levchenko TI, Nazemi A, Kaappa S, Malola S, Yousefalizadeh G, Calhoun LA, Stamplecoskie KG, Häkkinen H, Tsukuda T, Crudden CM (2019) Robust, Highly Luminescent Au₁₃ superatoms protected by N-heterocyclic carbenes. *J Am Chem Soc* 141:14997–15002. <https://doi.org/10.1021/jacs.9b07854>
 27. Rajamanikandan R, Ilanchelian M (2018) Protein-localized bright-red fluorescent gold nanoclusters as cyanide-selective colorimetric and fluorometric nanoproboscopes. *ACS Omega* 3:14111–14118. <https://doi.org/10.1021/acsomega.8b02044>
 28. Zheng J, Petty JT, Dickson RM (2003) High quantum yield blue emission from water-soluble Au₈ nanodots. *J Am Chem Soc* 125: 7780–7781. <https://doi.org/10.1021/ja035473v>
 29. Mathew A, Sajanlal PR, Pradeep T (2012) Selective visual detection of TNT at the sub-zeptomole level. *Angew Chem Int Ed* 51: 9596–9600. <https://doi.org/10.1002/anie.201203810>
 30. Kumar PP, Kaur N, Shanavas A, Neelakandan PP (2020) Nanomolar detection of biothiols via turn-ON fluorescent indicator displacement. *Analyst* 145:851–857. <https://doi.org/10.1039/C9AN02222H>
 31. Yen Y-T, Chen T-Y, Chen C-Y, Chang C-L, Chyueh S-C, Chang H-T (2019) A photoluminescent colorimetric probe of bovine serum albumin-stabilized gold nanoclusters for new psychoactive substances: cathinone drugs in seized street samples. *Sensors* 19: 3554–3564. <https://doi.org/10.3390/s19163554>
 32. Luo QJ, Li ZG, Lai JH, Li FQ, Qiu P, Wang XL (2017) An on-off-on gold nanocluster-based fluorescent probe for sensitive detection of organophosphorus pesticides. *RSC Adv* 7:55199–55205. <https://doi.org/10.1039/C7RA11835J>
 33. Goswami U, Sahoo AK, Chattopadhyay A, Ghosh SS (2018) In Situ synthesis of luminescent Au nanoclusters on a bacterial template for rapid detection, quantification, and distinction of kanamycin-resistant bacteria. *ACS Omega* 3:6113–6119. <https://doi.org/10.1021/acsomega.8b00504>
 34. Maity P, Sasai K, Dhital RN, Sakai H, Hasobe T, Sakurai H (2020) Excimer formation of aryl iodides chemisorbed on gold nanoparticles for the significant enhancement of photoluminescence. *J Phys Chem Lett* 11:1199–1203. <https://doi.org/10.1021/acs.jpcclett.9b03557>
 35. Chavda N, Trivedi A, Thakarda J, Agrawal YK, Maity P (2016) Size specific activity of polymer stabilized gold nanoparticles for transfer hydrogenation catalysis. *Catal Lett* 146:1331–1339. <https://doi.org/10.1007/s10562-016-1760-3>
 36. Tsunoyama H, Tsukuda T (2009) Magic numbers of gold clusters stabilized by PVP. *J Am Chem Soc* 131:18216–18217. <https://doi.org/10.1021/ja908188f>
 37. Sarina S, Waclawik ER, Zhu H (2013) Photocatalysis on supported gold and silver nanoparticles under ultraviolet and visible light irradiation. *Green Chem* 15:1814–1833. <https://doi.org/10.1039/C3GC40450A>
 38. Thomas SW, Joly GD, Swager TM (2007) Chemical sensors based on amplifying fluorescent conjugated polymers. *Chem Rev* 107: 1339–1386. <https://doi.org/10.1021/cr0501339>

Publisher's Note Springer Nature remains neutral with regard to jurisdictional claims in published maps and institutional affiliations.